View metadata, citation and similar papers at core.ac.uk

brought to you by CORE

provided by Kyutacar : Kyushu Institute of Technology Academic Repository

九州工業大学学術機関リポジトリ
Kyutacar
Kyushu Institute of Technology Academic Repository

Synthesis, characterization and its photoluminescence properties of group I-III-VI2 CuInS2 nanocrystals

著者	Oda Masaru, Miyaoka Tomotari, Yamada Shuhei, Tani Toshiro
journal or publication title	Physics Procedia
volume	29
page range	18-24
year	2012-06-09
URL	http://hdl.handle.net/10228/00006177

doi: info:doi/10.1016/j.phpro.2012.03.685

Available online at www.sciencedirect.com

SciVerse ScienceDirect

Physics Procedia 29 (2012) 18 – 24

Physics Procedia

16th International Conference on Luminescence

Synthesis, characterization and its photoluminescence properties of group I-III-VI_2 $CuInS_2$ nanocrystals

Masaru Oda[a,b,*], Tomotari Miyaoka[b], Shuhei Yamada[b], and Toshiro Tani[a,b]

[a] *Division of Advanced Applied Physics, Institute of Engineering,*
[b] *Department of Applied Physics, Graduate School of Engineering,*
Tokyo University of Agriculture and Technology, Naka-cho 2-24-16, Kogane-i, Tokyo 184-8588, Japan

Received 25 July 2011; accepted 25 August 2011

Abstract

We report the synthesis, characterization, and photoluminescence (PL) properties of colloidal I-III-VI_2 $CuInS_2$ and $CuInS_2$/ZnS nanocrystals (NCs). Absorption shoulder and PL bands of the NCs are located at higher energy than those of band gap energy of bulk crystals due to a quantum-confinement effect. The PL band has a relatively large Stokes-shift, broad linewidth, and long decay-time, which suggests that the PL originates from a recombination of confined-excitions associated with donor(s) and/or acceptor(s). We found that quantum yield of the PL depends strongly on the photon-energy of excitation light and that it is up to 40-50% in resonant excitation at the energy positions corresponding to the absorption shoulder. Detailed properties and possible dynamics will be described. We also present preliminary results of PL properties focused on single NCs. There exist high-luminescent NCs exhibiting so-called PL blinking as similar with II-VI NCs, while the others are dark NCs.
© 2012 Published by Elsevier B.V. Selection and/or peer-review under responsibility of the organizing committee represented by Stephen C. Rand and the guest editors. Open access under CC BY-NC-ND license.
PACS: 73.21.La, 78.47.jd, 78.67.Bf, 78.67.Hc

Keywords: nanocrystal; quantum dot; I-III-VI_2 compounds, photoluminescence; absorption; time-resolved measurement; single nanocrystals

1. Introduction

In recent years, colloidal II-VI CdSe/ZnS nanocrystals (NCs) [1,2] have been used in the field of chemistry, biology and life-science as a fluorescent labeling [3] in protein, DNA and cells due to their high photostability, wide absorption bands, and narrow and tunable photoluminescence (PL).

The NCs possess sufficiently high quantum yields of the PL (> 50 % @ room temperature), and so the PL from single NCs can also be observed by using a standard microscope system with a high-sensitive CCD camera. It has been reported that single NCs exhibit some remarkable PL properties, e.g. PL blinking [4,5] and polarized PL [6,7]. The single NCs are expected to be used as new types of functionalized probes by utilizing the remarkable properties. For example, PL blinking, i.e. on-off intermittency of PL intensity, is quite sensitive to the states of the NC surface [8], and thus it can be used as a sensitive probe of nano-environment. PL polarization measurements of single

* Corresponding author. Tel.: +81-42-388-7428; fax: +81-42-385-6255.
E-mail address: odamasa@cc.tuat.ac.jp

1875-3892 © 2012 Published by Elsevier B.V. Selection and/or peer-review under responsibility of the organizing committee represented by Stephen C. Rand and the guest editors. Open access under CC BY-NC-ND license.
doi:10.1016/j.phpro.2012.03.685

CdSe/ZnS NCs enable us to detect a direction of c-axis of each NC because the NCs possess two dimensional transition dipoles [6,7]. Thus real-time measurements of the PL polarization make it possible to investigate nanoscale dynamics of labeled molecules, e.g. torsional and rotational motion. While the PL properties of the NCs are quite attractive, the NCs have a problem especially for the biological uses that they contain toxic Cd-element.

Group I-III-VI_2 NCs are expected as one of the candidate materials of Cd-free NCs. The NCs are also fascinating because they have significantly large variation of band gap energy ranging from 1.23eV ($AgInSe_2$) to 3.49 eV ($CuAlS_2$). Particularly, the NCs with the band gap energies of near-infrared region have a great advantage for not only the biological use but also solar-cell applications. However, PL properties of the NCs have not been sufficiently elucidated; especially, there has no investigation on PL properties of single NCs as far as we know at preset. One of the reasons is that the synthesis of high-quality NCs is not so easy in the case of I-III-VI_2 NCs.

Recently, we have synthesized relatively high-quality I-III-VI_2 $CuInS_2$ NCs based on previous reports [9,10], and have formed ZnS shell around the $CuInS_2$ NCs. In this Letter, we will describe first the synthesis and characterization of the $CuInS_2$ NCs and $CuInS_2$/ZnS core-shell NCs, and then present detailed PL properties of the NCs including new results on single NCs.

2. Experimental

Chemicals. 99% copper(I) acetate and 99.99% indium(III) acetate are used as received from Strem Chemicals and Sigma-Aldrich Chemicals, respectively. 98% dodecanethiol, zinc stearate, 90% octadecene (ODE), 99% oleic acid and 99.5% acetone are purchased from Wako Chemicals, respectively. Pre-diluted dimethylzinc (Me_2Zn)/trioctylphosphine (TOP) solution (1:25 vol. ratio) is purchased from Trichemical Research.

Synthesis. The synthesis method of the $CuInS_2$ core-NCs is basically based on those in Refs [10, 11]. First, 24.4 mg (0.2 mmol Cu) copper acetate, 58.2 mg (0.2 mmol In) indium acetate, 0.5 mL dodecanethiol (2 mmol S) are mixed with 10 mL ODE in a 50 mL two-necked flask, and then 0.13 mL oleic acid (0.4 mmol) is added to prevent from aggregation of the NCs in the synthesis process. Then, the mixture is degassed under nitrogen gas flow for 30 minutes, and is subsequently heated to 240 °C with the rate of 8 °C per minutes. Next, the temperature is kept at 240 °C. In this paper, the duration time at 240 °C is defined as the reaction time. The heating and keeping resulted in nucleation and successive growth of the core-NCs.

The ZnS shells are formed around the $CuInS_2$ cores as follows. First, 0.13 mL Me_2Zn/TOP solution (0.06 mmol Zn) is mixed with 1 mL ODE, and then the mixture is charged into a syringe. Then the temperature of the flask containing the NC solution is cooled to 180 °C. Next, the mixed solution in the syringe is added dropwise with an interval of 30 seconds. After the addition, the temperature is cooled to 100 °C and kept for 2 hour for annealing. It is noted that using the purchased pre-diluted Me_2Zn/TOP solution reduces the risk due to pyrophoric nature of Me_2Zn in the synthesis. The prepared NCs are purified by precipitation with 5 mL acetone to rinse residual dodecanethiol, oleic acid, and ODE, and finally they are dispersed in anhydrous toluene solution.

Measurements. Absorption spectra were measured with a spectrometer (V-570, Jasco). PL and excitation spectra were recorded by using a modified spectrophotometer (FP-6500, Jasco). Transmission electron microscopy (TEM) images were taken with a transmission electron microscope (HF-2200, Hitachi). PL decay profiles were measured by a standard time-correlated single photon-counting method. A pulsed diode laser (LDH-PC405, Pico Quanta) was used as an excitation source. The light wavelength and pulse duration-time were 407.5 nm and 50 ps, respectively. We used a single photon-counting module (SPCM-AQRH, PerkinElmer), a time-to-amplitude converter (Ortec 567, EG&G) and also a multi-channel analyser (Ortec TRUMP-PCI-2K, EG&G) for the time-resolved measurements. Time resolution of the system is 600 ps. PL imaging of single NCs was performed under total internal reflection (TIRF) excitation configuration (see Fig. 4(a)) [12] by using an inverted-type optical microscope (TE-2000U, Nikon) with ×100, N.A. = 0.90 dry objective. We use 2D-CCD detector (Cascade-512B, Roper Scientific) for image acquisition; series of continuous images are obtained almost seamlessly (transfer rate: 1.024 ms/frame) with the exposure time for each frame of 100 ms. All the measurements were performed at room temperatures.

3. Results and Discussions

$CuInS_2$ NCs. First, we characterize optical and structural properties of the so-prepared $CuInS_2$ NCs. Figure 1(a) shows absorption spectra of the NCs dispersed in toluene solutions. Each spectrum is normalized at 3.0 eV. Reaction times of the NCs were 5, 10, 15, 30, 60 and 120 minutes, respectively. A broad shoulder appears at low energy side ranging from 1.7 to 2.2 eV in the spectra. The energy position of the shoulder shifts to red until 30 min, and then hardly shifts.

The inset of Fig. 1(a) shows a TEM image of $CuInS_2$ NCs with reaction time of 30 min. Individual particles show clear lattice patterns of which the lattice spacing is equals to that of bulk $CuInS_2$ crystals. It ensures that the particles are surely crystallized in chalcopyrite structure. The crystal shape looks angular, but it can be regarded as roughly spherical. The average diameter of the NCs was estimated to be 5.9 nm ± 1.4 nm.

The band gap energy due to the lowest state of the confined exciton in a spherical NC is expressed as [13],

$$E = E_g + (\hbar^2/2)\,(\pi/R)^2\,(1/\,m_e^{*} + 1/\,m_h^{*}) - 1.8e^2/\varepsilon R\,. \qquad (1)$$

where E_g, $\hbar$, R, m_e^{*}, m_h^{*}, e, and ε are band-gap energy of bulk $CuInS_2$ crystal (E_g = 1.54 eV), Dirac constant, radius of the NC, effective mass of electron ($m_e^{*} = 0.16m_0$), effective mass of hole ($m_h^{*} = 1.3m_0$), the elementary charge and the dielectric constant of the NC ($\varepsilon = 11\varepsilon_0$), respectively. It is noted that donors and acceptors are ignored in this model. In the case that the average diameter is equal to 5.9 nm ± 1.4 nm, the E is calculated to be 1.68-1.96 eV; though the value seems to be slightly small but roughly equals the energy of the absorption shoulder. The broadness of the absorption shoulder can be associated with size and shape distributions of the NCs.

It is also confirmed from results of a series of TEM observation that the particles grow monotonically until 30 min, and that the NCs hardly grow but its shape transforms from angular sphere to spheroid after 30 min. Thus the redshift until 30 min in the Fig. 1(a) can be explained basically in terms of quantum size effect. As for the lattice pattern of the NCs, it is ambiguous within the reaction time of 20 min, and after that it becomes clear quickly. This result suggests that the particles are rather amorphous at the first stage, and then in turn become crystalline.

Figure 1(b) shows corresponding PL spectra of the $CuInS_2$ NCs. Photon energy of the excitation light was 2.58 eV. Each NC solution was diluted so that its absorbance at 2.58 eV equalled to 0.04. The PL intensity increases gradually with redshift as the reaction time increases until 30 min, and then the intensity decreases.

Here, we describe the PL properties based on the results of PL decay measurements. The inset of Fig. 1(b) shows PL decay profiles of the NCs with the reaction time of 5 and 30 min, respectively. Main component of the profiles (green lines) has a time constant of several hundreds of nanosecond; it is one order of magnitude longer than that of CdSe NCs (15-30 ns). The long decay-time and also broad PL band with large Stokes shift suggest that the PL dynamics of the confined excitons in the $CuInS_2$ NCs should be associated with donors and/or acceptors in the NCs as similar to the case for bulk $CuInS_2$ crystals.

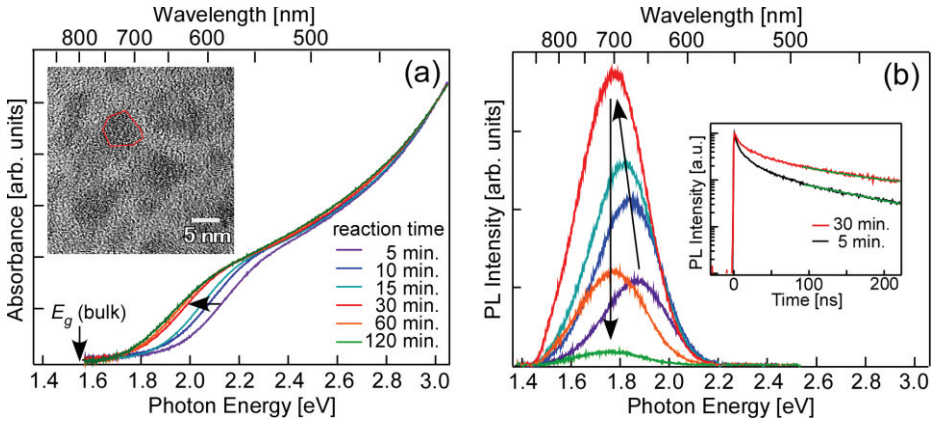

Fig. 1. Reaction time dependence of (a) absorption and (b) PL spectra of $CuInS_2$ NCs, respectively. The inset of Fig. 1(a) shows a TEM image of the NCs with reaction time of 30 min. Black and red lines in the inset of Fig. 1(b) show PL decay profiles of the NCs with reaction time of 5 and 30 min, respectively.

Intensity ratio of the main component increases monotonically with decreasing that of a fast component (tens of nanosecond) until 30 min. Assuming that the fast component arises from a competition between radiative and non-radiative recombination processes of carriers, the result can be described by a reduction of non-radiative recombination center(s) inside the NCs and/or on the NC surface. This interpretation is consistent with also the results in Fig. 1(b).

On the other hand, PL decay profiles hardly change after 30 min, though the PL intensity decreases drastically. It may suggest that part of the NCs becomes dark ones, i.e. such NCs emit fewer photons due to some reasons.

To investigate further details of optical properties of the ensemble $CuInS_2$ NCs, we measured excitation-energy (E_{ex}) dependence of PL spectra using the NCs with reaction time of 30 min as shown in Fig. 2. The excitation-energies corresponding to the individual spectra are indicated on the left side and also by arrows in the Fig. 2. PL band shifts to low energy side and the PL bandwidth decreases slightly as the excitation-energy decreases in the resonant region of $E_{ex} < 2.0$, while PL spectra show no dependence on excitation-energy in the nonresonant region of (2.9 >) $E_{ex} > 2.0$. In the case that the NCs are excited at the edge energy of the absorption shoulder (E_{ex} =1.8), the PL band shifts by 47 meV and the bandwidth is narrowed by 20 % as compared to those in the spectra at $E_{ex} > 2.0$.

The shift and narrowing suggest that the excitons in the lowest state described by eq. (1) are generated selectively by size in the region of $E_{ex} < 2.0$ as similar with the case of CdSe NCs. It is considered that almost all the NCs can be excited in the region of $E_{ex} > 2.0$ by generating not only the excitons in the lowest state but also those in the second or more higher states.

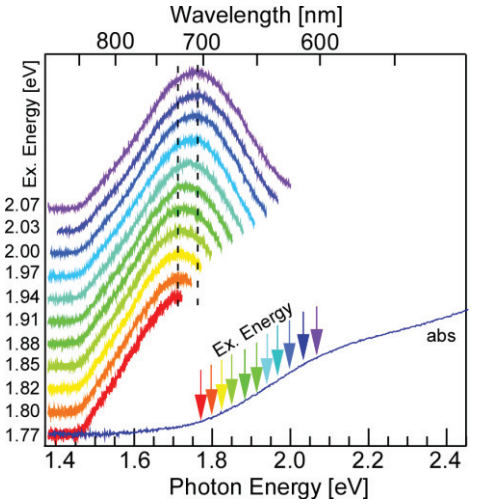

Fig. 2. Excitation-energy dependence of PL spectra of the $CuInS_2$ NCs with reaction time of 30 min.

$CuInS_2$/ZnS core-shell NCs. Next, we describe optical properties of $CuInS_2$/ZnS core-shell NCs. It is known that PL quantum yield of CdSe NCs increases due to formation of ZnS shell [11]. The band gap of CdSe lies within that of ZnS energetically, and so both electrons and holes are confined inside the CdSe-core, mainly. The confinement can prevent the carriers from approaching non-radiative centers on the NC surface. Thus a similar effect can be expected for the $CuInS_2$ NCs because its band gap also lies within that of ZnS.

Red, green and blue lines in the Fig. 3(a) show PL spectra of $CuInS_2$ NCs, $CuInS_2$/ZnS NCs without and with 1 hour heat-annealing, respectively. The PL intensity increases roughly twice by the formation of the ZnS shell as expected. PL quantum yields were estimated to be 4.8, 6.6 and 7.7 % at E_{ex} = 2.34 eV (530 nm), respectively, and they were kept at least for two weeks. It is noted that we also tried to form ZnS shell by using other starting materials, i.e. zinc stearate and zinc acetate, instead of Me_2Zn. In these cases, similar increasing of the PL intensity can be achieved, but the PL quantum yields decreased drastically after few days.

PL peak energy shifts to high energy side by 37 meV due to the shell formation as shown in Fig. 3, while it shifts low energy side slightly in the case of CdSe NCs because the confinement effect is reduced due to a penetration of the wavefunctions of carriers from core to shell.

The blue shift can be described as follows. In our previous study on CdSe/ZnS NCs, we found that the NCs which

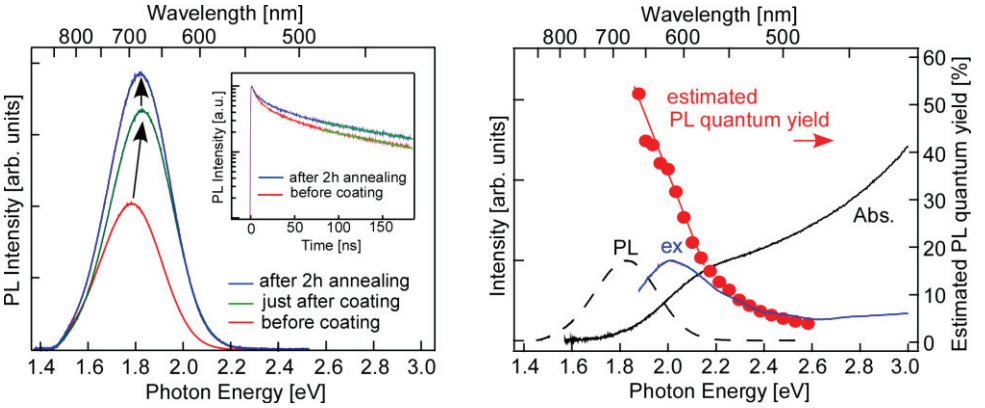

Fig. 3. (a) PL increase due to ZnS shell formation. Red, green and blue lines show PL spectra of non-coated $CuInS_2$ NCs, coated $CuInS_2$/ZnS NCs jut after the shell formation, and also the coated NCs followed by the 100 °C annealing for 2 hour, respectively. Red and blue lines in the inset show PL decay profiles of the non-coated NCs and the coated NCs followed by the annealing, respectively.
(b) Black solid, broken, and blue lines show absorption, PL and excitation spectra. Red circles show PL quantum yield of the NCs calculated by using the Eq. (2).

possess local charges on the NC surface show redshift by tens of meV, and that the redshift disappears due to neutralization of the charges by photo-adsorption of polar-molecules, e.g. water and ammonia molecules [14], on to NC surface. Assuming that there are local charges on the surface of the $CuInS_2$ NCs, observed blueshift can be interpreted that the charges are neutralized by the shell formation. The origin of the charges is considered to be dangling bonds on the NC surface.

Red and blue lines in the inset of Fig. 2 show PL decay profiles of the $CuInS_2$ and the annealed $CuInS_2$/ZnS NCs. Intensity ratio of the main component increases due to the shell formation with decreasing that of a fast component. Decay time of the main component show no change as shown in green lines. These results can be explained by considering a reduction of non-radiative recombination centers corresponding to the dangling bonds on the NC surface.

Black solid, broken and blue lines in Fig. 3(a) show absorption, PL and excitation spectra of the $CuInS_2$/ZnS NCs, respectively. The PL spectrum was measured under excitation at E_{ex} = 2.34 eV, and the excitation spectrum was monitored at the peak energy of the PL band. It is notable that the excitation spectrum shows a sharp peak at the energy of the absorption shoulder, and the spectral shape is quite different from that of absorption spectrum especially at higher energy.

Here, we consider excitation-energy dependence of PL quantum yields in the $CuInS_2$/ZnS NCs. The PL quantum yield $Q(E_{ex})$ were calculated by using the measurement value of the quantum yield at the E_{ex} = 2.34 eV ($\equiv E_0$) and the equation shown below,

$$Q(E_{ex}) = (E_{ex}/E_0)\left[(1\text{-}10^{-A(E_0)})/(1\text{-}10^{-A(E_{ex})})\right](N(E_{ex})/N(E_0))\,Q(E_0) \quad (2)$$

where $A(E_{ex})$ and $N(E_{ex})$ are absorbance at E_{ex} and total photon number of PL per unit time at E_{ex}, respectively. We used here the approximation $N(E_{ex})/N(E_0) \cong I(E_{ex})/I(E_0)$, where the $I(E_{ex})$ is the PL intensity per unit time at the PL peak energy shown in Fig 3(b) (1.82eV). This approximation is correct in the case that there exists no excitation-energy dependence of the shape of PL spectra. Thus it is exactly correct under the condition of nonresonant excitaion because no dependence appears as similar with the case of $CuInS_2$ NCs (Fig. 2). It is noted that the error is estimated to be at most 10% (totally 10% overestimation; 20% overestimation due to PL narrowing and 10% underestimation due to spectral redshift) even under resonant excitation because the spectral change is not so large.

Red circles in Fig. 3(b) show the quantum yield $Q(E_{ex})$ which was calculated by using Eq. 2. We found that the quantum yields of the $CuInS_2$/ZnS NCs depend strongly on the photon-energy of the excitation light; the quantum

yield increases gradually with decreasing photon energy, and finally reaches up to 40-50%. The maximum value in the resonant excitation region is comparable to that of luminescent CdSe/ZnS NCs. These results may suggest that non-radiative recombination tend to occur when photo-generated carriers relax from higher to the lower states or that there is a pathway from higher states to something like a dark state.

Note that the quantum yields of non-coated $CuInS_2$ NCs also show the similar strong dependence, and thus its origin may be associated with donors and/or acceptors in the NC cores.

PL properties of single NCs. To get further insight into the optical properties of the $CuInS_2$/ZnS NCs, and also to explore specific PL properties of single NCs, we have been measuring the PL from single NCs by utilizing a total internal fluorescence (TIRF) microscopy method (Fig 4 (a) [12]).

For the measurements, the NCs were first dispersed in toluene solution, and then were expanded onto a silica glass substrate with a hydrophobic surface by spin-casting. We adjusted the concentration of the NC solution to be 1×10^{-7} mol/L. It is noted that the concentration is one or two orders of magnitude higher than that in our study on single CdSe/ZnS NCs because we could detect only fewer particles in the PL measurements in the case of $CuInS_2$/ZnS NCs.

Figure 4(b) is an enlargement of a PL image of the $CuInS_2$/ZnS NCs under 532 nm light excitation, and Figs. 4 c1-c5 show typical time trajectories of PL intensity from each bright spot observed in the PL image. The c2 and c5 correspond to the trajectories at A and B in Fig. 4(b), respectively. It is turned out that PL blinking, i.e. on-off intermittency of PL intensity appears also in the I-III-VI_2 QDs as shown in Figs. 4 c1-c4. The blinking behaviour is associated with the occasional events of capturing and releasing of photogenerated carriers at trap sites on or near NC surface [4,5].

On the other hand, the time trajectory shown in Fig. 4 c4, PL intensity increases twice at around 27 seconds, and so the PL is considered to be from two (or more) NCs. In the case of spot B, spot size seems to be slightly larger than that of diffraction limited size (ca. 470 nm), and its PL trajectory (c5) shows no on-off intermittency. Thus, the trajectory is considered to be composed of PL from several NCs.

From such careful examinations of the time trajectories for each blight spot, we found that that the PL intensity during the on-events per unit time of the single NCs is ranging roughly from half to a third as compared with that of CdSe/ZnS NCs and that the occurrence of the on-off intermittency seems to be basically similar (stochastic analysis should be needed for more quantitative comparison). Though these NCs are sufficiently luminescent, there are also many dark NCs of which the PL intensity is difficult to distinguish from background signal in the PL image.

Two possible reasons can be considered at present. The first one is that a few NCs are resonantly excited by the 532 nm light irradiation and the NCs can emit photons quite effectively as can be seen in Fig. 3 (b), while

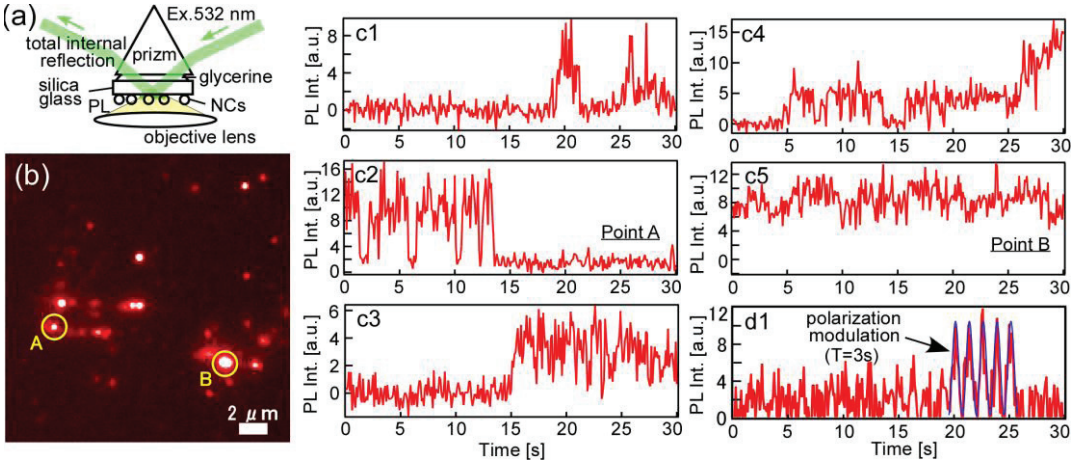

Fig. 4. (a) TIRF excitation configuration of the PL imaging measurement [12]. (b) PL image of the $CuInS_2$/ZnS NCs (enlargement of a CCD image of 512×512 pixels). Figs. c1-c5 show the examples of PL time trajectories of each bright spot observed in the CCD image. Fig. d1 shows a typical PL time trajectories under linear-polarization modulation of the PL with rotation speed of 1/3 Hz.

nonresonant NCs hardly emit photons. Second one is that all of the NCs are excited nonresonantly, but there are two types of NCs; one type is high-luminescent, and the other is dark NCs. We will be measuring excitation-energy dependence of the PL blinking of single $CuInS_2$/ZnS NCs to elucidate the reason.

Finally, we present a preliminary result of a polarization modulation measurement of single NCs, though further investigation is needed for discussing the polarized properties of the NCs. The PL from single NCs was analysed by using a rotating linear-polarizer with a frequency of 1/3 Hz. Figure 4 d1 shows one of the trajectories in the measurement. PL modulation with the rotation frequency can be observed in the time range between 20 s to 25 s, i.e. during duration time of a PL on event. This result indicates that PL of single $CuInS_2$/ZnS NCs is polarized. Detailed properties of the PL polarization of the $CuInS_2$/ZnS NCs will be described elsewhere with quantitative analysis.

4. Smmary

In summary, we have synthesized group I-III-VI_2 $CuInS_2$ NCs and $CuInS_2$/ZnS core-shell NCs, and characterize the optical properties of the NCs. In absorption spectra, broad shoulder appears at low energy side of the spectra. Based on the results of TEM observations, the shoulder is assigned as due to exciton absorption confined in the NCs, and the origin of the broadness of the shoulder is large size and shape distribution of the NCs. As for the PL intensity, strong dependence on the reaction-time was observed. The PL process in the $CuInS_2$ NCs is considered to be dominated by the relaxation process associated with donors/acceptors inside the NCs. The PL decay measurement confirms that the exciton PL is surely affected by the donors/acceptors as similar with the case of bulk $CuInS_2$ crystals.

We have investigated the effects on PL properties of the NCs by ZnS shell formation. As a results, PL quantum yield increases from 4.8 % to 7.7 %, and the value is kept at least for two weeks. We found that the PL quantum yield of the NCs depends strongly on the photon-energy of the excitation light, and the value is up to 40-50%. In addition, we have succeeded to detect PL from single NCs. It is turned out that there are two types of $CuInS_2$/ZnS NCs; one is sufficiently luminescent NCs as similar with II-VI NCs, and the other is too dark NCs.

Acknowledgements

This work is partly supported by grants-in aid from Ministry of Education, Science, Sports and Culture, Nos. 22710086 / 23651105.

References

[1] C. B. Murray, D. J. Norris, and M. G. Bawendi, *J. Am. Chem. Soc.*, **115**, 8706 (1993).
[2] X. Peng, E. Troy, A. Wilson, A. P. Alivisatos, *Angew. Chem. Int. Ed. Engl.*, **36**, 45 (1997).
[3] W. C. W. Chan and S. Nie, *Science*, **281**, 2016 (1998).
[4] M. Nirmal, B. O. Dabbousi, M. G. Bawendi, J. J. Macklin, J. K. Trautman, T. D. Harris, and L. E. Brus, *Nature*, **383**, 802 (1996).
[5] M. Kuno, D. P. Fromm, S. T. Johnson, A. Gallagher, and D. J. Nesbitt, *Phys. Rev*. **B67**, 125304 (2003).
[6] J. Sepiol, J. Jasny, J. Keller, U. P. Wild, *Chem. Phys. Lett.*, 273 444 (1997).
[7] I. Chung, K. T. Shimizu, M. G. Bawendi, *Proc. Natl. Acad. Sci. USA*, 100 405 (2003).
[8] M. Oda, A. Hasegawa, N. Iwami, K. Nishiura, N. Ando, A. Nishiyama, H. Horiuchi, and T. Tani, *J. Lumin.*, 127, 198 (2007).
[9] H. Zhong, Y. Zhou, M. Ye, Y. He, J. Ye, C. He, C. Yang, and Y. Li, *Chem. Mater* 20 6434 (2008).
[10] R. Xie, M. Rutherford, and X. Peng, *J. Am. Chem. Soc.* 131, 5691 (2009).
[11] M. A. Hines, P. G. Sionnest, *J. Phys. Chem.* 100, 468 (1996).
[12] T. Tani, M. Oda, K. Mashimo, F. Tachibana and H. Horiuchi, *J. Lumin*. 119-120 173 (2006).
[13] L. Brus, *J. Phys Chem*, 90, 2555 (1986).
[14] M. Oda, J. Tsukamoto, A. Hasegawa, N. Iwami, K. Nishiura, I. Hagiwara, N. Ando, H. Horiuchi and T. Tani, *J. Lumin.* 119-120, 570 (2006).